Signals of Opportunity for Car Density Estimation with Limited Training Data

Wesam Al Amiri, Omar Abdelsalam, James T. Jones, Terry N. Guo and Allen B. MacKenzie

Abstract—Passive sensing leverages existing signals from illuminators of opportunity to perform target localization, detection, and tracking without the need for additional infrastructure. In this paper, we explore the use of WiFi signals of opportunity for estimating car density in parking lots. The aim is to develop an efficient and cost-effective parking occupancy estimation system to alleviate traffic congestion caused by drivers searching for parking spaces. To achieve this, experimental measurements were conducted in a real outdoor environment to collect reflected WiFi signals from targets (cars). These collected signals were then used for car density estimation using a combination of semisupervised learning convolutional neural network (CNN) and weighted-centroid interpolation techniques, only requiring small size datasets and limited measurements. The proposed method overcomes the limitations of existing data-driven estimators by reducing the reliance on large labeled datasets and computational complexity associated with traditional supervised learning methods. In addition, it provides a cost-effective alternative to the traditional systems that rely on a large number of sensors. Simulations are performed to evaluate the performance of the estimation, and the results demonstrate that our scheme can effectively estimate car densities in the parking lot with reasonable estimation errors.

Index Terms—WiFi signals of opportunity, passive bistatic radar (PBR), environment monitoring, car density estimation, semi-supervised learning, convolutional neural network (CNN).

-3559-0/23/$31.00 ©2023 IEEE | DOI

I. Introduction

Passive bistatic radar (PBR) has gained significant attention in recent years as an effective method for localizing, detecting, and tracking targets [1]. It can also make use of various ambient communication signals of opportunity, including frequency modulation (FM) signals [2], digital video broadcasting terrestrial (DVB-T) signals [3], global system for mobile communication (GSM) signals [4], orthogonal frequency division multiplexing (OFDM) signals [5], and WiFi signals [6]. PBR offers several advantages over traditional radar systems, including cost reduction, stealth capabilities, compact size, and minimal interference to existing wireless systems, as it does not require a dedicated radar transmitter.

With the widespread deployment of WiFi infrastructure in residential, commercial, and industrial areas, WiFi signals have become a valuable resource for passive sensing in both indoor and outdoor environments through fingerprinting techniques [7], [8], [9]. WiFi fingerprinting techniques have been extensively used in indoor positioning and sensing systems. For example, in [7] WiFi fingerprints were used to detect human presence and classify human activity using support vector machine (SVM) by analyzing Doppler information. In [8] a fast and reliable method was proposed for collecting WiFi fingerprints in indoor environments to enable accurate indoor localization. In [9] the authors presented a WiFi fingerprintingbased indoor localization method using dynamic mode decomposition (DMD) feature selection and hidden Markov model (HMM). These advancements in indoor WiFi fingerprinting have inspired researchers to explore the potential of WiFi signals of opportunity for sensing in outdoor applications, particularly in intelligent transportation system (ITS). Utilizing WiFi signals of opportunity for sensing in ITS can greatly enhance real-time data collection, analysis, and decisionmaking processes for effective traffic management in urban areas. In particular, WiFi sensing can make a significant impact in managing traffic congestion caused by drivers searching for vacant parking spaces in crowded cities. Research indicates that approximately 30 percent of traffic congestion is attributed to parking search activities [10]. By leveraging WiFi's sensing capabilities, real-time information on parking lot car density can be collected and analyzed. This information allows for the estimation of parking space availability. Subsequently, this data can then be used to effectively direct drivers to vacant parking lots, leading to improved traffic flow, reduced traffic congestion, and a positive environmental impact [11]. WiFi signals of opportunity provides a cost-effective alternative to existing parking occupancy detection systems that rely on numerous sensors for real-time occupancy monitoring. These systems often require substantial implementation and maintenance costs. Also, vision-based systems, which rely on cameras, often face performance limitations when operating in challenging environmental conditions such as low lighting, fog, and snow [12].

In an effort to overcome these challenges, some researchers have utilized radio-based fingerprinting techniques with deep supervised learning for estimating parking availability [13]. However, employing deep supervised learning for such systems often requires huge labeled datasets, which can be resource-intensive, time-consuming, and demanding in terms of effort. These requirements may not be feasible in many practical scenarios, limiting the adoption and application of various deep learning methods [14].

To address these issues, this paper presents a low-cost yet effective scheme that utilizes WiFi signals of opportunity as fingerprints for estimating car density in parking lots. The

W. Al Amiri, J.T. Jones and A.B. MacKenzie are with the Dept. of Electrical and Computer Engineering, Tennessee Technological University, Cookeville, TN (email: waalamiri42, jtjones49, amackenzie {@tntech.edu}). O. Abdelsalam is with the Dept. of Computer Science, Tennessee Technological University, Cookeville, TN (email: oabdelsal42@tntech.edu). T.N. Guo is with the Center for Manufacturing Research, Tennessee Technological University, Cookeville, TN (email: nguo@tntech.edu).

979-8-3503-3559-0/23/$31.00 ©2023 IEEE

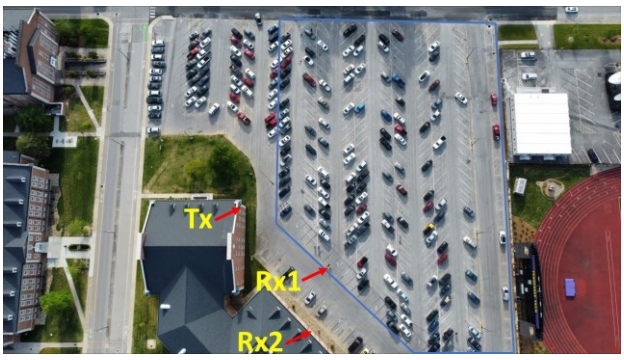

Fig. 1: The environmental layout of Tennessee Tech University parking lot in which the experiment was performed and the locations of the transmitter and receivers used in the experiment.

estimation process involves the use of a semi-supervised learning combined with weighted-centroid interpolation techniques to mitigate the reliance on large labeled datasets. First, we developed an effective measurement approach to collect both the direct path signal and reflected signals from targets within the desired area of interest using a Universal Software Radio Peripheral (USRP) software-defined radio (SDR) platform.

In particular, we constructed two receivers employing USRP X300 devices, as illustrated in Figure 1. These receivers were strategically positioned to capture signals transmitted by the WiFi access point (Tx) and subsequently reflected from the targets located within the parking lot. The receiver (Rx1) was dedicated to capture the direct path signal, while the other receiver (Rx2) was utilized for capturing the echo signal. Data collection in the parking lot was conducted for a limited number (L) of occupancy scenarios, for instance, three different levels: empty, moderate, and full. Next, a deep semi-supervised learning framework was developed to infer the status of a parking lot based on raw samples obtained from the receivers. Our focus was on using semi-supervised learning to classify spectrograms of the raw samples, which provide insights about car density. The aim of utilizing semi-supervised learning is to reduce the reliance on extensively annotated datasets, thereby improving the efficiency and effectiveness of the classification process [15]. Then, we employed the weighted-centroid method to estimate the number of cars in the parking lot, where the semi-supervised learning classification accuracy used as the weights in this estimation process. Finally, simulations were conducted to evaluate the performance of the semi-supervised learning approach and the weighted-centroid. The performance evaluations indicate that our proposed scheme can estimate the number of cars in a parking lot with reasonable estimation error and relatively small size datasets.

The rest of this paper is organized as follows. Section II presents related work. The experiment and dataset preparation are presented in Section III. The proposed scheme is described in Section IV. Performance evaluations and numerical results are discussed in Section V, followed by conclusions in Section VI.

II. Related Work

Current parking occupancy detection can be categorized into three main types: wireless sensor network (WSN) solution [16], [17], crowd monitoring solution [18], [19], and visionbased solution [12], [20].

WSN solutions typically involve deploying individual sensor nodes for each parking space. The commonly utilized sensor types include magnetic, ultrasonic, infrared, and loop sensors. These WSN-based detection algorithms are generally known for their high efficiency [16], [17]. However, they are susceptible to false detections in specific situations. For instance, magnetic sensors can be influenced by the presence of large nearby metallic objects, like a truck in an adjacent parking space. Ultrasonic and infrared sensors can be affected by environmental factors such as weather conditions and lighting variations, leading to potential inaccuracies in detection. Furthermore, these WSN solutions often require a large number of sensors to cover the parking area effectively.

The crowd monitoring-based parking occupancy detection [18], [19] often involve the use of sensors integrated into mobile phone applications or probe vehicles. These approaches rely on crowdsensing strategies to gather information on urban parking availability. They can be seen as an alternative to traditional static parking sensors. However, their practicality is still limited to certain scenarios. Firstly, the cost associated with these methods can be quite high, as it necessitates a

high deployment of sensors, such as probe vehicles, to gather sufficient parking information. Secondly, while this strategy is effective for detecting on-street parking in urban areas, it may not be suitable for large parking lots where the number of moving sensors inside the parking lot is limited.

The vision-based solution utilizes cameras with artificial intelligence for parking occupancy detection [12], [20]. For instance, in [12], the authors proposed a visual detection system for parking space occupancy that utilizes a CNN. The system takes an image of a single parking spot as input and performs the detection task. Although the scheme achieved very high accuracy, its performance rapidly degrades in bad weather environments and poor lighting conditions.

To address the challenges faced by existing systems, some researchers [13] have proposed the integration of radio-based fingerprinting systems as a backup solution for camerabased systems, particularly in scenarios where vision-based approaches encounter difficulties. By utilizing radio-based sensing and localization techniques, the proposed system aims to provide accurate and reliable parking lot detection, and occupancy monitoring. However, the paper lacks in-depth experimental validation or practical implementation of the proposed approach.

Different from existing parking occupancy detection systems, we exploit the signals of opportunity transmitted

from WiFi access points (APs) to estimate the car density in campus parking lots. The proposed methodology is based on hardware experiments and it is unaffected by poor lighting and can adapt to bad weather conditions. Furthermore, unlike current systems that rely on supervised-learning CNN approaches and require huge labeled datasets, our approach does not necessitate exten-

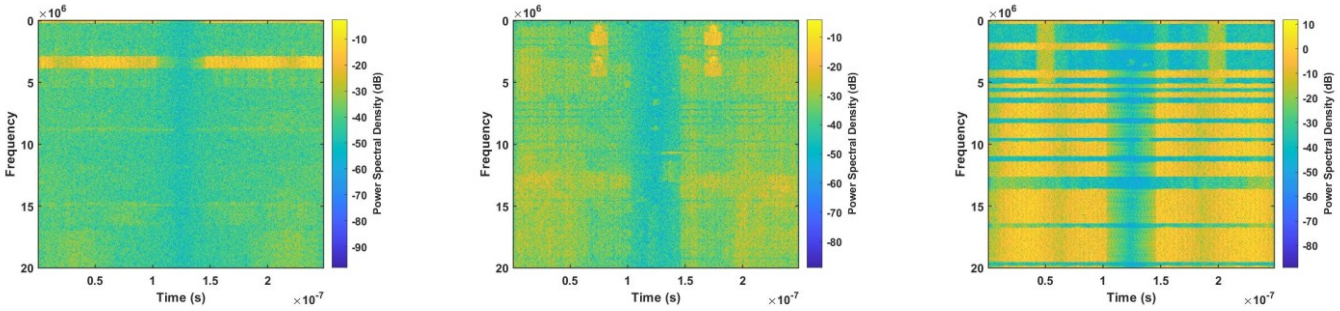

(a) (b) (c)

Fig. 2: Spectrogram of segments from collected signals: (a) empty parking scenario; (b) moderate-density parking scenario; (c) full-density parking scenario.

sive datasets or high computational complexity for accurately estimating parking availability.

III. Experiment and Data Set Preparation

A. Experiment Setup

The experiment setup is shown in Fig. 1, where USRPs used to capture signals from the WiFi AP installed on the wall of Tennessee Tech Library. The heights of the WiFi AP, Rx1, and Rx2 are 6 meters, 2 meters, and 6 meters, respectively. The WiFi AP provides coverage for an area of approximately 8646 square meters, including 282 parking spaces indicated by the blue line in Fig. 1. Signals were collected at different WiFi frequency bands, namely 2.437 GHz, 5.240 GHz, 5.580 GHz, and 5.785 GHz.

Multiple rounds of experiments were conducted to generate datasets that contain car-density information. The desired signals are those reflected by the cars. There are a few challenges to capture stable and relevant datasets: 1) the opportunistic signals are not under our control, and the signal power is affected by the number of users and data traffic so that it fluctuates randomly; 2) it is practically impossible to capture pure reflected signals, and what we can get is a mix of signals coming from different directions; and 3) extracting the reflected signals from a composite of signals is difficult. To combat the randomness and reduce the impact of disturbing factors, we consider measuring the reflected signal power relative to the background signal power. Each round of experiment includes two measurements for a particular density, labeled as "Σ" and "bg" (short for "background"), respectively. Ideally, measurement "Σ" tries to capture the reflected signals by using a horn antenna pointing to the cars in the parking lot, while the other one tries to record all other signals excluding the reflected signals. Practically, each recording contains a mix of many signals (downlink signals from the AP, uplink signals from user equipment (UE), and signals reflected from objects (buildings and cars, etc.).

B. Dataset Preparation

Let $S_{\Sigma}^{(n)}(t)$ and $S_{bg}^{(n)}(t)$ be the measured waveforms after some process (e.g., time-domain gating and frequency-domain filtering to cut off unrelated parts in the mixed signals), corresponding to the two types of experiments, respectively; where index n, $n = 1,2,\cdots,N$, refers to car density levels of interest, with $n = 0$ and $n = N$ for empty and full occupant scenarios, respectively. Roughly speaking, $S_{\Sigma}^{(n)}(t)$ contains two terms and can expressed as

$$S_{\Sigma}^{(n)}(t) \approx S_{ref}^{(n)}(t) + \alpha S_{bg}^{(n)}(t-\tau), \quad (1)$$

where $S_{ref}^{(n)}(t)$ is the signal reflected from the cars, and α is an unknown positive number together with a delay τ representing a fraction of unwanted background signal mixed with the desired element. It is reasonable to say that the wideband signals $S_{ref}^{(n)}(t)$ and $S_{bg}^{(n)}(t-\tau)$ are mostly uncorrelated, which leads to the following relation of average signal powers, corresponding to $S_{\Sigma}^{(n)}(t)$ $S_{ref}^{(n)}(t)$ and $S_{bg}^{(n)}(t-\tau)$:

$$\bar{P}_{\Sigma}^{(n)} \approx \bar{P}_{ref}^{(n)} + \alpha^2 \bar{P}_{bg}^{(n)}. \quad (2)$$

As an effort to reduce the impact of signals that are uncorrelated to the car density, we decide to use the relative power of the two types of measured signals, i.e., generate datasets using $S_{\Sigma}^{(n)}(t) \Big/ \sqrt{\bar{P}_{bg}^{(n)}}$. Specifically, spectrograms which are obtained by applying short-time Fourier transform to $S_{\Sigma}^{(n)}(t) \Big/ \sqrt{\bar{P}_{bg}^{(n)}}$ are used as input data for our approach. Fig. 2 shows the spectrogram of selected segments from collected signals under different parking lot occupancy scenarios, where full-density and moderate-density correspond to 282 and 126 cars, respectively. Spectrograms offer a useful representation of the signal, showcasing the relationship between instantaneous frequency and time as a non-negative function. They are also valuable for estimating the power spectral density of the signal, which can be utilized to infer car density.

The spectrogram generation process involves dividing the recorded signal into segments, with each segment containing 100,000 samples. These segments are then transformed into spectrograms. The resulting spectrograms for different densities serve as inputs to a CNN that employs image-based classification techniques. This CNN is trained using the semisupervised learning algorithm, utilizing 1,500 spectrograms as training inputs. Once the CNN has been trained using these spectrograms, it can be employed to classify spectrograms of signals with unknown car densities into the predefined classes. The CNN utilizes its learned features and patterns to make predictions and assign the unknown spectrograms to

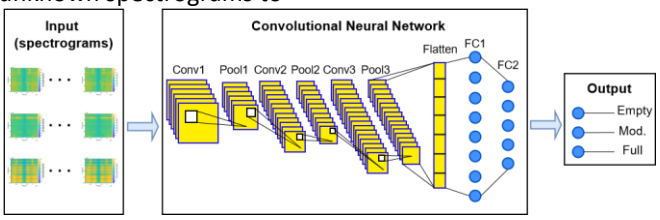

Fig. 3: The structure of the proposed CNN.

the appropriate car density class. This classification process, combined with the weighted-centroid technique, enables the estimation of car densities.

IV. Estimation Using CNN With Spectrograms

We have developed a CNN architecture that utilizes spectrotemporal data, i.e., spectrograms, obtained from a WiFi AP and USRP X310 SDR testbed. Inspired by the architecture of AlexNet [21], which was originally designed for image classification tasks, our proposed CNN architecture, depicted in Fig. 3, has been modified to suit our specific application. Unlike AlexNet, our CNN architecture comprises 3 convolutional layers, 3 max pooling layers, and 2 fully connected layers. The proposed CNN is lightweight and less computationally expensive compared to AlexNet. The input to the CNN consists of multiple segmented sequences of raw IQ samples represented as graphical spectrograms with a size of 224 × 224 pixels. This is then fed to the first convolution layer (Conv1). The convolution layer consists of spatial filters, called kernels, which perform a convolution operation over input data to extract the features. It applies 64 filters to extract features from the input using the Rectified Linear Unit (ReLU) activation function. In order to decrease the size of the feature maps generated by Conv1, we employ a max pooling layer (Pool1). Superficially, It downsamples the feature maps, effectively reducing the number of parameters and controlling overfitting. Then, this layer is connected to the second convolution layer (Conv2), where it performs another convolution operation with 128 filters to capture higher-level features in the spectrogram. Conv2 is connected to another max pooling layer (Pool2) to further reduce the spatial dimensions of the feature maps obtained from Conv2. Next, convolution layer 3 (Conv3) conducts another convolution operation with 256 filters to extract more complex and abstract features from the spectrogram. Another max pooling layer (Pool3) further downsamples the feature maps from Conv3. To prepare the features for classification, we employ a flatten layer that reshapes the output of the previous layer into a 1D vector. The flattened features are then passed to the first fully connected layer (FC1) consisting of 1024 units, where the ReLU activation function is applied to compute a nonlinear transformation. Similarly, the second fully connected layer (FC2) layer also comprises 1024 units with ReLU activation. It further processes the transformed features. Overall, our CNN architecture combines convolutional layers for feature extraction, max pooling layers for downsampling, and fully connected layers for high-level feature processing and classification. These architectural components are tailored to our specific application and dataset. Table III summarizes the architecture of our CNN model.

TABLE I: Architecture of the proposed CNN.

Layer Type	Layer Name	# of Units	Activation Function
Input	Input	224 × 224 × 3	-
Convolutional	Conv1	64	ReLU
Max Pooling	Pool1	-	-
Convolutional	Conv2	128	ReLU
Max Pooling	Pool2	-	-
Convolutional	Conv3	256	ReLU
Max Pooling	Pool3	-	-
Flatten	Flatten	-	-
Fully Connected	FC1	1024	ReLU
Fully Connected	FC2	1024	ReLU
Output	Output	3	Softmax

To train and evaluate the proposed CNN, L (≥ 2) distinct datasets representing L different car density levels are collected. By analyzing the spectrograms using our CNN, we harness its robust image recognition capabilities to infer the density of cars in the parking lot.

After collecting the datasets and generating spectrograms, we employ a semi-supervised learning approach with CNN to train the datasets. The idea is to utilize L labeled datasets, as well as an unlabeled dataset with an unknown number of cars, which will be classified to the pre-defined L classes. In this paper, the labeled datasets representing empty, moderate, and full densities.

Subsequently, the unlabeled dataset can be preprocessed by generating spectrograms for the unknown number of cars. Without considering the labels, the trained CNN model is employed to extract features from the unlabeled spectrograms. These extracted features are then subjected to a clustering algorithm (e.g., k-means) which assigns cluster labels to the unlabeled data based on the clustering results.

Finally, the trained CNN model can be employed to classify and test the unknown dataset into empty, moderate, or full categories based on the labeled data. Then, the weightedcentroid can be used to estimate the number of cars for the unknown dataset. Specifically, we calculate the weights for each class based on their accuracies generated by the CNN. The weights can be calculated as the ratio of each class accuracy to the sum of all accuracies. Denote the validation accuracies as A_i, where $i = 0,1,\cdots,L$ refers to L predetermined density levels at which datasets are prepared. Given an unknown dataset as the input to an L-class classifier, it outputs L accuracy scores that can be used as weights for weight-centroid interpolation. Then, the weighted centroidbased car density estimate can be calculated as follows:

$$\tilde{N}_v = \frac{\sum_{i=0}^{L} A_i * N_{v(i)}}{\sum_{i=0}^{L} A_i} \tag{3}$$

where $\tilde{N}_v$ is the estimated number of cars and $N_{v(i)}$ is the real number of cars of the ith class during dataset collection. Note that the adoption of a semi-supervised approach enables us to leverage a larger quantity of unlabeled data alongside a smaller set of labeled data during the training process. This approach reflects a more realistic scenario, considering the challenges involved in collecting and labeling extensive volumes of data. By utilizing unlabeled data effectively, we can enhance the training process and improve the model's performance even with limited labeled data available. Moreover, the use of weighted-centroid reduces the need of huge datasets for estimating the number of cars.

TABLE II: Confusion matrix of the proposed classifier.

		Predicted		
		Empty	Full	Total
True	Empty	80	6	86
	Full	1	103	104
	Total	81	109	190

V. Performance Evaluation and Numerical Results

In this section, we assess the effectiveness of the proposed car density estimation method for parking lots. Three (L = 3) car density levels are considered for evaluation: empty, moderate and full, corresponding to 0, 126 and 282 cars. To evaluate its performance, we use the dataset representing the moderate density class as the dataset with an unknown number of cars, while the other datasets (empty and full) serve as benchmarks for estimating the number of cars.

A. Performance Metrics

To evaluate the performance of the proposed CNN-based model, we considered the following metrics. The accuracy (A_i) was calculated by considering the moderate data as input to a binary classifier (full vs empty). This metric yields two separate accuracy values, which can be calculated based on the classification of positives and negatives as follows:

$$A_i = \frac{TP + TN}{TP + TN + FP + FN} \tag{4}$$

where TP, TN, FP, and FN represent true positive, true negative, false positive, and false negative, respectively.

The detection rate (DR) measures the percentage of scenarios that are estimated correctly and it is given as:

$$DR = \frac{TP}{TP + FP} \tag{5}$$

The $\mathbf{F_1}$ score provides a balanced measure of both precision and recall. It can be given as:

$$F_1 = \frac{TP}{TP + \frac{1}{2}(FP + FN)} \tag{6}$$

The false acceptance rate (FA) measures the percentage of scenarios that are falsely estimated and it is represented as:

$$FA = \frac{FP}{TN + FP} \tag{7}$$

The highest difference (HD) is the difference between DR and FA.

$$HD = DR - FA \tag{8}$$

TABLE III: Proposed semi-supervised learning model performance evaluation results.

Class	$\mathbf{A_i}$%	DR %	$\mathbf{F_1}$%	FA %	HD %
Empty	0.93	0.90	0.91	0.06	0.84
Full	0.78	0.62	0.76	0.34	0.28

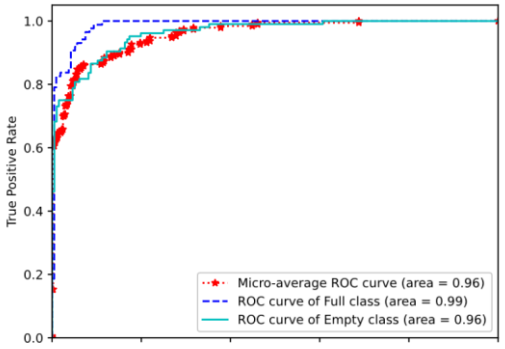

Fig. 4: The ROC curve of the semi-supervised learning model.

The receiver operating characteristic (ROC) curve is used to evaluate the accuracy of the classifier, which is measured by the area under the curve (AUC). This area indicates how much the model can distinguish between the classes, where a higher AUC represents a better performance.

Finally, the evaluation of weighted-centroid performance is using the root mean square error deviation ($RMSD$) which can be represented as follows:

$$RMSD = \sqrt{\frac{\sum_{t=1}^{T}(\tilde{N}_{v_t} - N_{v_t})^2}{T}} \quad (9)$$

where $\tilde{N}_{vt}$ is the estimated number of cars at iteration t, N_{vt} is the real number of cars, and T is the number of iterations.

B. Numerical Results

To evaluate the semi-supervised learning CNN model, we divided each dataset into training and validation sets. Subsequently, we utilized the proposed CNN model on the spectrograms and assessed its performance using the evaluation metrics mentioned in Subsection V-A . We used the confusion matrix given in Table II to find the values of TP, TN, FP and FN, and then calculate the values of the performance metrics. The results are summarized in Table III. Note that the semisupervised learning approach achieved an average accuracy of 85.5%. In addition, Fig. 4 shows the ROC curve for the proposed CNN using the empty and full datasets.

After evaluating the proposed CNN model, we applied the weighted-centroid based on (3) to estimate the number of cars of the moderate density. The weighted-centroid estimator leads to an estimate $\tilde{N}_v = 129$, which is close to the real number of cars 126. Then, the calculated RMSD of the car density estimator over several iterations is equal to 6.51.

Finally, we compare the proposed scheme with some of the existing parking density estimation schemes [12], [13].

TABLE IV: Comparison of parking density estimation schemes.

	Radio-based	Average accuracy	Bad weather	Size of dataset	Complexity
[12]	× √	97.7%	× √	huge	high
[13]	√	91%	√	huge	high
Ours		85.5%		small	low

Scheme [12] achieves highest estimation accuracy, however it is based on cameras and the accuracy degrades rapidly during bad weather conditions. Scheme [13] is based on cameras and it uses radio signals in bad weather conditions. It achieves higher accuracy compared to our scheme. However, both schemes [12], [13] require huge labeled datasets and high computational resources, which contribute to the increased complexity of the estimation scheme.

VI. Conclusions and Future Work

In this work, we proposed and tested a particular use case of performing radio-based car density estimation in parking lots. The proposed scheme exploits the WiFi signals of opportunity and fingerprinting to provide an efficient and cost-effective alternative to current parking occupancy detection systems. It makes use of the combination of semi-supervised learning CNN and weighted-centroid interpolation to estimate the car density with limited measurements and relatively small labeled datasets. The performance evaluation and simulation results demonstrate that the proposed scheme can efficiently estimate car densities in parking lots with reasonable estimation errors. The proposed approach adapts to bad weather conditions and eliminates the need for extensive labeling efforts and complex processing typically associated with traditional supervised learning techniques.

While the proposed methodology aims to reduce the complexity of existing car density estimation schemes, there are certain limitations and issues that require further investigation. For example, the correlation between the presence of WiFi users and the estimation accuracy is not clear and needs to be investigated. Additionally, the recorded signals contain a mixture of various signals, including downlink signals, uplink signals, and reflected signals. Some signal separation techniques, like blind source separation, may be considered to extract desired signals.

In the future, we will consider extracting strongly-relevant information and apply data fusion from multiple WiFi APs for increased performance. Additionally, we aim to conduct tests under a wider range of parking lot scenarios. Furthermore, incorporating additional labeled data and introducing more classes will be considered to further improve the accuracy and effectiveness of the results.

Overall, the proposed method provides a possible mechanism to reduce the dataset size and system computational complexity for real-time applications utilizing radio-based fingerprinting. These findings have practical implications for different real-time applications that uses radio-based fingerprinting that requires low complexity and high processing speeds, such as traffic management of self-driving autonomous vehicles, health applications, etc.

Acknowledgment

This work is supported by the National Science Foundation under grant #2135275.

References

[1] Z. Wang, Q. He, and R. S. Blum, "Exploiting information about the structure of signals of opportunity for passive radar performance increase," *IEEE Transactions on Signal Processing*, vol. 69, pp. 6083–6100, 2021.

[2] F. Maasdorp, J. Cilliers, and C. Tong, "Propeller modulation analysis of 4-blade, 4-engine aircraft in FM-band multistatic passive radar," in *proc. of IEEE International Radar Conference (RADAR)*, 2020.

[3] T. Martelli, F. Colone, and R. Cardinali, "DVB-T based passive radar for simultaneous counter-drone operations and civil air traffic surveillance," *IET Radar, Sonar & Navigation*, vol. 14, no. 4, pp. 505–515, 2020.

[4] B. Knoedler, M. Broetje, and W. Koch, “A particle filter for trackbefore-detect in GSM passive coherent location,” in *proc. of IEEE Radar Conference (RadarConf)*, 2019.

[5] Y. Li, X. Wang, and Z. Ding, “Multi-target position and velocity estimation using OFDM communication signals,” *IEEE Transactions on Communications*, vol. 68, no. 2, pp. 1160–1174, 2019.

[6] W. Li, R. J. Piechocki, K. Woodbridge, C. Tang, and K. Chetty, “Passive wifi radar for human sensing using a stand-alone access point,” *IEEE Transactions on Geoscience and Remote Sensing*, vol. 59, no. 3, pp. 1986–1998, 2020.

[7] W. Li, B. Tan, and R. J. Piechocki, “WiFi-based passive sensing system for human presence and activity event classification,” *IET Wireless Sensor Systems*, vol. 8, no. 6, pp. 276–283, 2018.

[8] F. Gu, M. Ramezani, K. Khoshelham, X. Zheng, R. Zhou, and J. Shang, “Fast and reliable wifi fingerprint collection for indoor localization,” *arXiv preprint arXiv:2009.03743*, 2020.

[9] O. P. Babalola and V. Balyan, “WiFi fingerprinting indoor localization based on dynamic mode decomposition feature selection with hidden markov model,” *Sensors*, vol. 21, no. 20, p. 6778, 2021.

[10] T. Giuffre, S. M. Siniscalchi, and G. Tesoriere, “A novel architecture of` parking management for smart cities,” *Procedia-Social and Behavioral Sciences*, vol. 53, pp. 16–28, 2012.

[11] D. N. C. Loong, S. Isaak, and Y. Yusof, “Machine vision based smart parking system using internet of things,” *Telkomnika (Telecommunication Computing Electronics and Control)*, vol. 17, no. 4, pp. 2098–2106, 2019.

[12] S. Nurullayev and S.-W. Lee, “Generalized parking occupancy analysis based on dilated convolutional neural network,” *Sensors*, vol. 19, no. 2, p. 277, 2019.

[13] M. Bauhofer, Y. Zhang, M. Arnold, and S. Ten Brink, “6G radio-based parking lot detection,” in *proc. of IEEE 3rd International Symposium on Joint Communications & Sensing (JC&S)*, 2023.

[14] Y. Ouali, C. Hudelot, and M. Tami, “An overview of deep semisupervised learning,” *arXiv preprint arXiv:2006.05278*, 2020.

[15] Q. Zhang and W. Saad, “Semi-supervised learning for channel chartingaided IoT localization in millimeter wave networks,” in *proc. of IEEE Global Communications Conference (GLOBECOM)*, 2021.

[16] F. Al-Turjman and A. Malekloo, “Smart parking in IoT-enabled cities: A survey,” *Sustainable Cities and Society*, vol. 49, p. 101608, 2019.

[17] T. Lin, H. Rivano, and F. Le Mouel, “A survey of smart parking¨ solutions,” *IEEE Transactions on Intelligent Transportation Systems*, vol. 18, no. 12, pp. 3229–3253, 2017.

[18] A. Khan, J. Ali Shah, K. Kadir, W. Albattah, and F. Khan, “Crowd monitoring and localization using deep convolutional neural network: A review,” *Applied Sciences*, vol. 10, no. 14, p. 4781, 2020.

[19] U. Singh, J.-F. Determe, F. Horlin, and P. De Doncker, “Crowd monitoring: State-of-the-art and future directions,” *IETE Technical Review*, vol. 38, no. 6, pp. 578–594, 2021.

[20] R. Ke, Y. Zhuang, Z. Pu, and Y. Wang, “A smart, efficient, and reliable parking surveillance system with edge artificial intelligence on iot devices,” *IEEE Transactions on Intelligent Transportation Systems*, vol. 22, no. 8, pp. 4962–4974, 2020.

[21] G. E. Hinton, A. Krizhevsky, and I. Sutskever, “ImageNet classification with deep convolutional neural networks,” *Advances in neural information processing systems*, vol. 25, no. 1106-1114, p. 1, 2012.